Stress buildup in the Himalaya

L. Bollinger,[1,2] J. P. Avouac,[2,3] R. Cattin,[3] and M. R. Pandey[4]

Received 26 November 2003; revised 16 July 2004; accepted 5 August 2004; published 20 November 2004.

[1] The seismic cycle on a major fault involves long periods of elastic strain and stress accumulation, driven by aseismic ductile deformation at depth, ultimately released by sudden fault slip events. Coseismic slip distributions are generally heterogeneous with most of the energy being released in the rupture of asperities. Since, on the long term, the fault's walls generally do not accumulate any significant permanent deformation, interseismic deformation might be heterogeneous, revealing zones of focused stress buildup. The pattern of current deformation along the Himalayan arc, which is known to produce recurring devastating earthquakes, and where several seismic gaps have long been recognized, might accordingly show significant lateral variations, providing a possible explanation for the uneven microseismic activity along the Himalayan arc. By contrast, the geodetic measurements show a rather uniform pattern of interseismic strain, oriented consistently with long-term geological deformation, as indicated from stretching lineation. We show that the geodetic data and seismicity distribution are reconciled from a model in which microseismicity is interpreted as driven by stress buildup increase in the interseismic period. The uneven seismicity pattern is shown to reflect the impact of the topography on the stress field, indicating low deviatoric stresses (<35 MPa) and a low friction (<0.3) on the Main Himalayan Thrust. Arc-normal thrusting along the Himalayan front and east-west extension in southern Tibet are quantitatively reconciled by the model. *INDEX TERMS:* 7230 Seismology: Seismicity and seismotectonics; 8164 Tectonophysics: Stresses—crust and lithosphere; 8158 Tectonophysics: Plate motions—present and recent (3040); 8102 Tectonophysics: Continental contractional orogenic belts; 9320 Information Related to Geographic Region: Asia; *KEYWORDS:* seismic cycle, interseismic, microseismicity, geodesy, Himalaya, Nepal

Citation: Bollinger, L., J. P. Avouac, R. Cattin, and M. R. Pandey (2004), Stress buildup in the Himalaya, *J. Geophys. Res.*, *109*, B11405, doi:10.1029/2003JB002911.

1. Introduction

[2] Large earthquakes are thought to rupture fault patches that have remained partially or fully locked for a period of time long enough for elastic stresses to reach the value needed to overcome friction on the fault. Determining the geometry of the locked portion of an active fault, the proportion of slip taken up by seismic ruptures and the seismic coupling ratio, are therefore major issues in seismotectonics. These questions can be addressed through geodetic measurements and have been investigated along a number of subduction zones [*Freymueller et al.*, 2000; *Hyndman and Wang*, 1993; *Mazzotti et al.*, 1999; *Oleskevich et al.*, 1999; *Prawirodirdjo et al.*, 1997; *Savage*, 1983]. Along-strike variations in elastic strain can result from lateral variations in the geometry of the locked fault zone and from unsteady loading during the interseismic period. Variations in elastic strain may therefore reveal stress buildup around major asperities [*Dmowska et al.*, 1996] or result from postseismic relaxation [*Freymueller et al.*, 2000]. In the case of an intracontinental megathrust, such as along the Himalaya, heterogenous interseismic strain may be detected from the pattern of microseismicity as well as from geodetic measurements. Indeed, it seems that in this setting, interseismic stress buildup controls the spatial distribution of background seismicity [*Cattin and Avouac*, 2000]. Interseismic strain along the Himalayan arc probably vary laterally, in particular at the transition between the $\sim$300 km arc segment, east of Kathmandu, that produced the 1934 $M \sim 8.2$ earthquake, and a long-standing seismic gap west of Kathmandu [*Bilham et al.*, 2001] where the last major event may date back to about 500 yr ago. The uneven microseismic activity along the Himalayan arc is a possible indication of an heterogeneous pattern of stress buildup. This pattern might be taken to reflect the arc segmentation in terms of large earthquakes, or to the influence of the north-south grabens in southern Tibet. We address these questions, taking advantage of the significant efforts made over the last ten years in geodetic

[1]Commissariat à l'Energie Atomique, Laboratoire Détection et Géophysique, Bruyères le Châtel, France.
[2]Geological and Planetary Sciences Division, California Institute of Technology, Pasadena, California, USA.
[3]Laboratoire de Géologie, Ecole Normale Supérieure, Paris, France.
[4]Department of Mines and Geology, National Seismic Centre, Kathmandu, Nepal.

0148-0227/04/2003JB002911$09.00

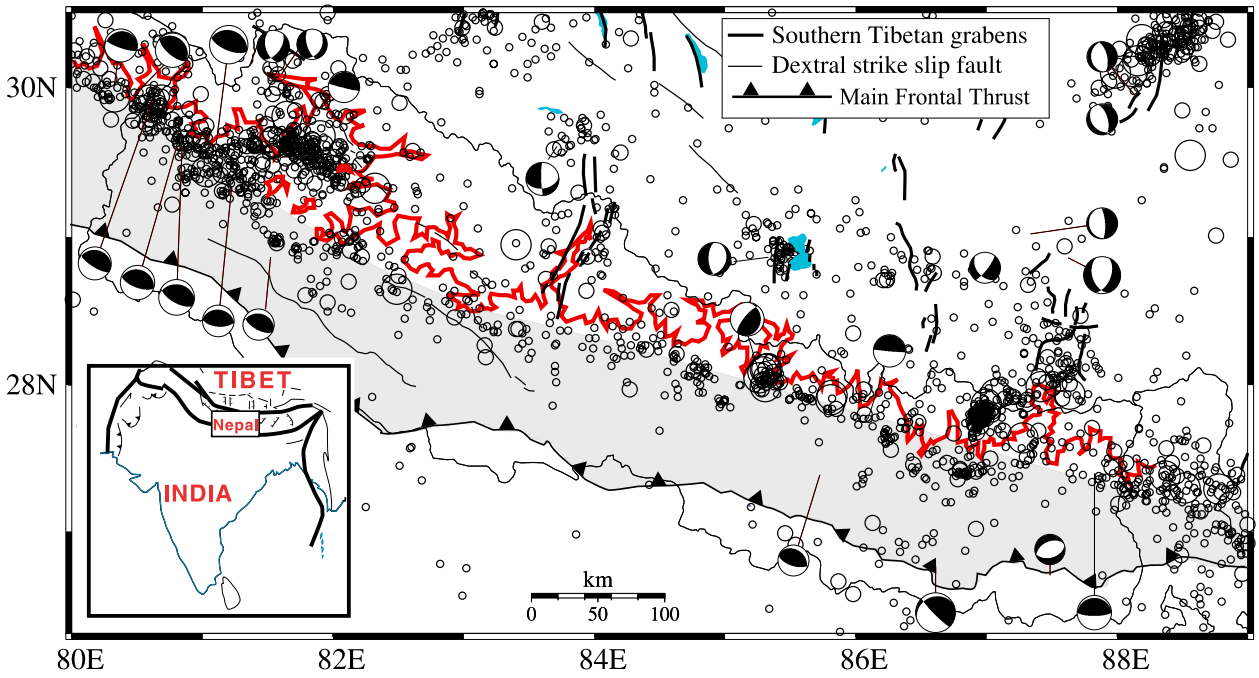

Figure 1. Microseismicity recorded between 1 April 1995 and 11 April 2000 by Nepal Seismological Center, Department of Mines and Geology (DMG). Only events with magnitude above $M\mathrm{l}$ = 3.0, well above the detection threshold of the network [*Pandey et al.*, 1999], are shown. Focal mechanisms are from *Baranowski et al.* [1984], *Chen and Kao* [1992], *Molnar and Chen* [1983], *Molnar and Lyon-Caen* [1989], *Ni and Barazangi* [1984], B. Kumar (DMG, personal communication, 1998), and the Harvard Centroid Moment Tensor (CMT) catalog. The grey band and red line present the assumed location of the locked portion of the fault with a downdip edge at 15 km and the location of the 3500 m contour line (DEM-Gtopo30/USGS), respectively.

[*Bilham et al.*, 1997; *Jouanne et al.*, 2004, 1999; *Larson et al.*, 1999] and seismic monitoring [*Pandey et al.*, 1995, 1999].

2. Seismotectonics of the Himalayan Megathrust

[3] In central western Nepal, crustal deformation is mostly localized on a single major fault, the Main Himalayan Thrust fault (MHT) [*Cattin and Avouac*, 2000; *Lavé and Avouac*, 2000]. The MHT emerges along the Himalayan piedmont, where it is known as the Main Frontal Thrust Fault (MFT) [*Nakata*, 1989], and roots some 100 km farther north into a subhorizontal ductile shear zone. This zone of probably ductile flow [*Cattin and Avouac*, 2000], coincides with a prominent midcrustal reflector at ~35 km depth revealed by seismic experiments in southern Tibet [*Zhao et al.*, 1993]. On the long-term average, all of the crustal shortening across the range is taken up by 21.5 ± 1.5 mm/yr slip along this megathrust [*Lavé and Avouac*, 2000]. Geodetic measurements over the last decade indicate that the fault south of the ductile region has remained essentially locked [*Bilham et al.*, 1997; *Jouanne et al.*, 2004, 1999; *Larson et al.*, 1999] while its downdip continuation is creeping at a rate comparable to the geological slip rate. Intense microseismic activity is triggered by stress accumulation at the downdip edge of the locked fault [*Cattin and Avouac*, 2000], resulting in a seismic belt that can be traced laterally along the front of the high range in Nepal [*Pandey et al.*, 1999] (Figure 1). Since most interseismic strain in the upper crust is ultimately converted to slip on the MHT, fault slip occurring between and during large earthquakes must sum up over the long term to a rather uniform distribution. There is no information on coseismic deformation due to the 1934 event, but it is highly probable that this earthquake ruptured a portion of the MHT with some heterogeneous slip distribution, as generally observed for major earthquakes [*Lay and Kanamori*, 1981]. Some analogy might be drawn in particular with the 1999 Chichi earthquake in Taiwan, which occurred on a shallow thrust fault, fully locked from the surface to a depth where it roots to a subhorizontal ductile shear zone. This event ruptured only a fraction of the previously locked fault [*Dominguez et al.*, 2003] with a rather heterogeneous slip distribution [*Huang*, 2001; *Johnson et al.*, 2001]. Significant, post seismic afterslip [*Hsu et al.*, 2002] was not sufficient to smooth out coseismic heterogeneities or allow to a full transfer of the strain that accumulated downdip of the locked fault portion.

[4] Given that the megathrust at the front of the Himalaya or along the western flank of the Central range in Taiwan are silent in the interseismic period, two possibilities arise. One is that the fault remains fully locked during the interseismic period and coseismic slip distributions during successive events would sum up to a uniform cumulative slip distribution. Another possibility is that strain over a significant fraction of the interseismic period is heteroge-

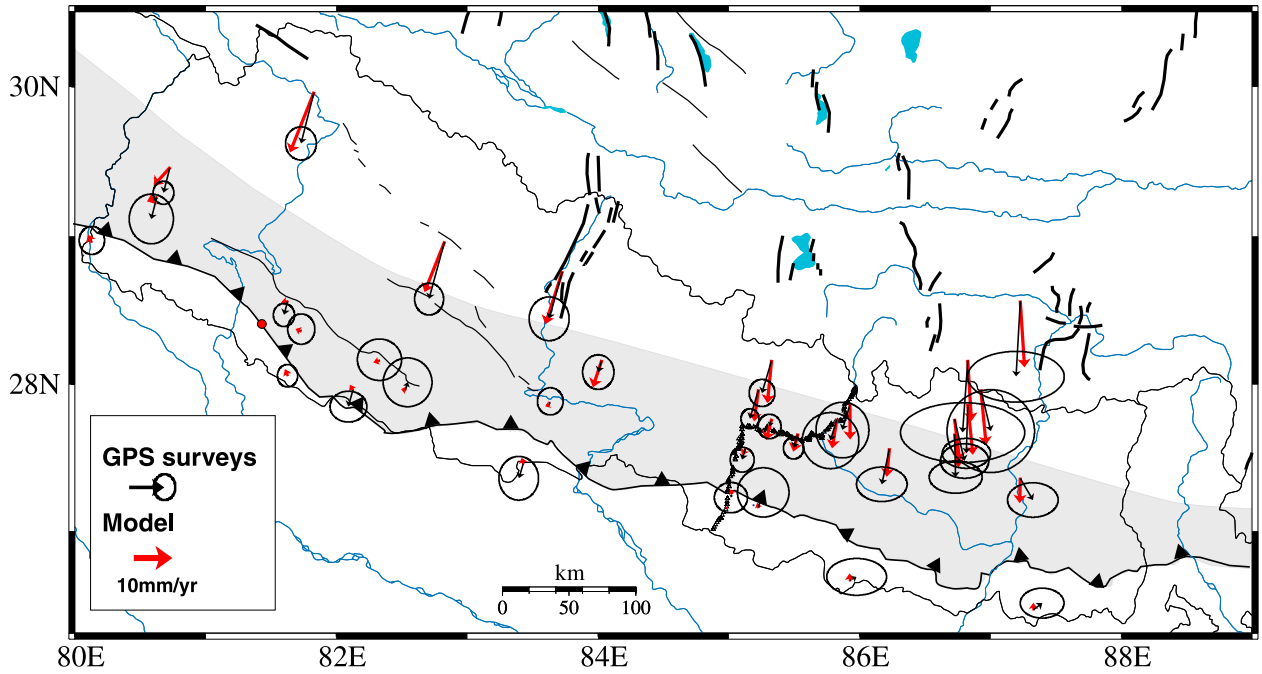

Figure 2. Observed and modeled geodetic displacement rates. Global Positioning System (GPS) data from *Jouanne et al.* [2004] and *Larson et al.* [1999] were registered to ITRF97 and ITRF94, respectively. The two data sets have 11 stations in common, and most of the campaigns were realized simultaneously by the two groups. The differences between the two data sets are therefore most probably due to the choice of different ITRF systems and different solutions for the motion of India. The two data sets differ essentially by a translation of 5 mm/yr in the north-south direction and −0.5 mm/yr in the east-west direction. In this representation, velocities are shown with respect to India, as defined by *Jouanne et al.* [2004] and the data of *Larson et al.* [1999] where expressed in the same reference frame by correcting for the translation between the two sets. Modeled velocities were computed assuming 19 mm/yr of slip along a subhorizontal (5°N) creeping zone with an upper tip at 17 km depth. We use the *Okada* [1992] formulation for point sources in an elastic half-space with elastic moduli $\lambda = \mu = 0.33.10^{11}$ N/m^2. The spacing between nodes is about 30 s along the front of the high Himalayas and increases farther north (up to 5 min under Tibet).

neous due to persistent asperities, possibly with a structural origin, that remain locked while some fault patches creep continuously, or intermittently during transient nonseismic events. To test these possibilities we have analyzed jointly seismicity and geodetic data available along the Nepal Himalaya.

3. Modeling Geodetic Deformation and Seismicity Along the Himalaya: A Fully Locked Seismogenic Zone

[5] Geodetic data [*Jackson and Bilham*, 1994; *Jouanne et al.*, 2004; *Larson et al.*, 1999] collected across the Nepal Himalayas were compiled and registered to a common reference frame (Figures 2, 3a, and 3b). The data were next modeled by three-dimensional (3-D) forward model of interseismic strain in which the subhorizontal ductile shear zone is approximated by a creeping dislocation embedded in an elastic half-space. This approach has been shown to be a reliable approximation both in terms of ground displacements at the surface and interseismic stress variations [*Vergne et al.*, 2001]. To take into account the geometry of the arc and possible lateral heterogeneities, we use a 3-D formulation for point source dislocations [*Okada*, 1992]. For comparison with microseismic activity along the range front, Coulomb stress variations [*King et al.*, 1994] were computed at a depth of 10 km, which is typical of hypocentral depths in this area. We first assumed a uniform regional stress field (Figure 4). A fully locked fault zone was assumed and the geometry of the downdip edge of the locked zone was adjusted so to fit the geometry of the seismicity belt (Figure 1) as well as geodetic displacements (Figures 2, 3a, and 3b). The thrusting direction remains perpendicular to the arcuate mountain front (see auxiliary material[1]), as indicated from focal mechanism (Figure 1). This simple model provides a satisfying fit to the GPS data (Table 1) with a χ^2 of 1.22. This means that there are no along-strike variations in interseismic strain that can be resolved by the geodetic data, within the uncertainty on these data. The model predicts a zone of increased Coulomb stress that coincides spatially with the belt of seismicity along the high range front (Figure 4). Owing to the slightly diverging thrusting induced by the arcuate shape of the range, this model induces along strike stretching of the overhanging wall, consistent with the location of the major grabens north of the Himalaya (Figure 5). Some complex-

[1]Auxiliary material is available at ftp://ftp.agu.org/apend/jb/2003JB002911.

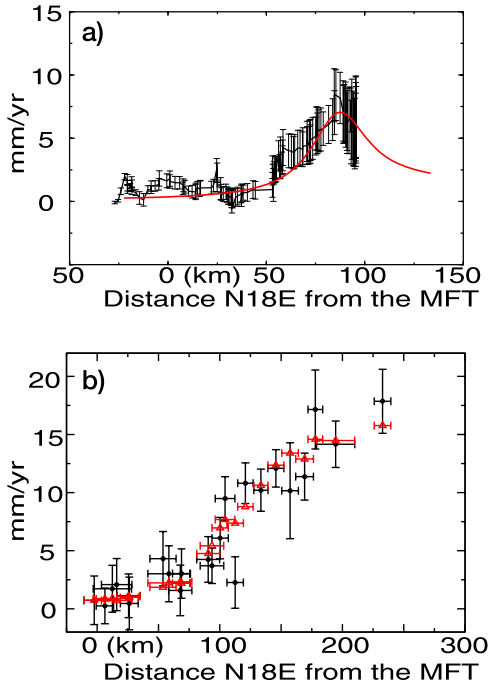

Figure 3. Interseismic velocities along the Himalayan front relative to India. (a) Observed [*Jackson and Bilham*, 1994] and modeled vertical displacements along the leveling line across the Kathmandu basin. See Figure 2 for the location of the leveling line. (b) Observed and modeled horizontal velocities projected on a N18°E section.

ities in the distribution of seismicity are not well reproduced and could be taken to suggest a more complex geometry of the downdip edge of the locked fault. An example of this may be the prominent cluster of seismicity in westernmost Nepal (from 81°E to 82°E). Uneven seismicity may reflect subtle lateral variations not visible from the existing geodetic data. Alternatively, it could reflect spatial variations of the regional stress field.

4. Influence of Topography on Stress Field: Evidence for Low Deviatoric Stresses and Low Friction on the Himalayan Megathrust

[6] We observe that the seismic activity correlates with the geometry of the front of the high range. If areas where north-south grabens intersect with the Himalayan arc are excluded, the seismicity becomes abruptly extinct as elevation gets higher than about 3500 m, so that the seismicity more or less follow the sinuous geometry of this elevation contour line. These observations may reflect the influence of the topography on the stress field. The stress field obviously varies with the topography. It changes from north-south thrusting south of the high Himalaya to east-west extension north of the high range (Figure 1). The seismicity cut off corresponding to the 3500 m elevation probably indicates the point where Coulomb stresses no longer increase, or perhaps actually decrease, during the interseismic period. To test the topographic control on seismicity we have computed Coulomb stress variations due to interseismic strain that account for topographic modulation of the stress field (Figure 6). If the deviatoric stresses at the front of the high range are small enough that the stress regime becomes extensional in southern Tibet,

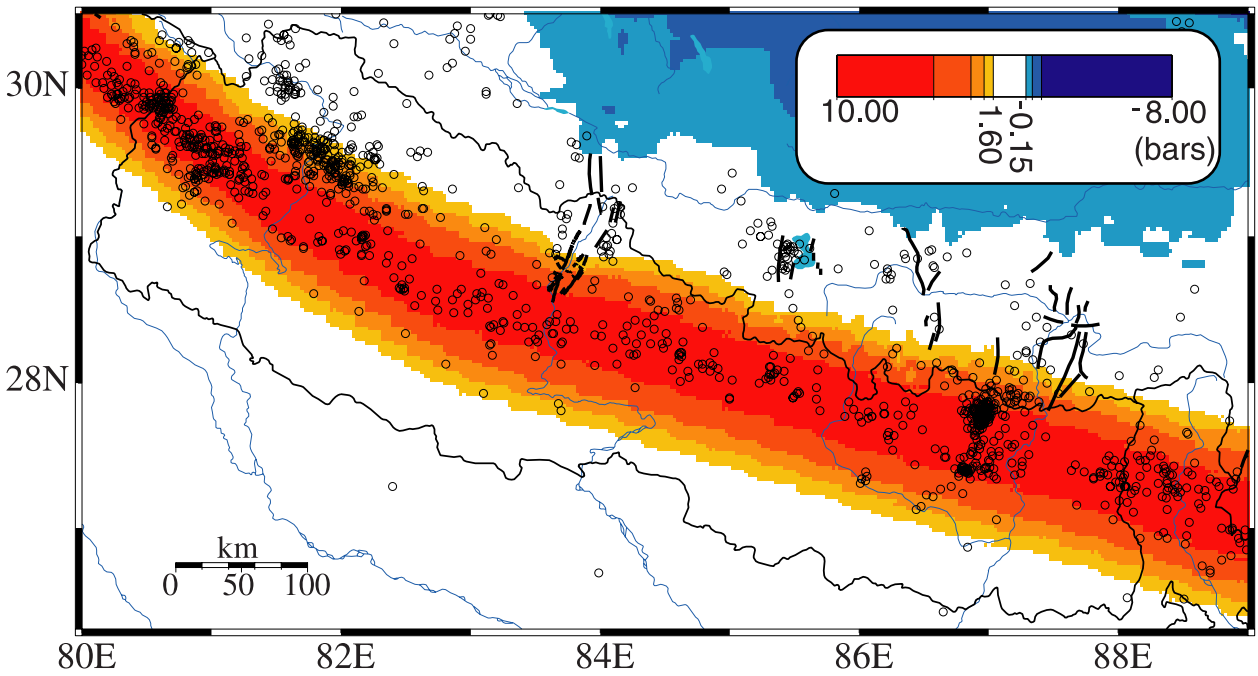

Figure 4. Stress accumulation rate along the Himalayan front during the interseismic period. Coulomb stress variations were computed assuming a uniform regional stress field with σ_1 striking N18°E and $\Delta\sigma = 250.10^6$ Pa.

Table 1. Weighed Mean Squares, $\chi^2 = 1/n\ (\Sigma((\text{Vob} - \text{Vcal})/\sigma))^2$, Computed From Comparing Modeled (Vcal) and Observed (Vob) Displacement Rates[a]

	Set 1 [*Larson et al.*, 1999], ITRF94	Set 2 [*Jouanne et al.*, 2004], ITRF97	Mixed Set
χ^2 north	1.006506	2.417458	1.883143
χ^2 east	0.623334	0.694165	0.612105
χ^2 total	0.776114	1.521238	1.22843
Translation (N/E), mm	−3.3/+0.9	2.0/0.0	2.0/0.0
Ref. frame	ITRF94-NNRA (each point)	India [*Jouanne et al.*, 2004]	India [*Jouanne et al.*, 2004]
Translation (N/E), mm	−3.3/+0.9	2.0/0.0	2.0/0.0

[a]Where σ is the uncertainty on Vob at the 67% confidence level. Various subsets of data were considered to test the relative contributions to the total misfit of the north-south and east-west components and the possible uneven contribution from the two sources of data [*Jouanne et al.*, 2004; *Larson et al.*, 1999]. The last line lists the translations applied to bring the velocities of *Larson et al.* [1999], expressed with respect to India in the ITRF94-NNRA reference frame, and those of *Jouanne et al.* [2004], expressed with respect to India into ITRF 97, that minimized the residuals between the computed and observed displacement rates.

then the effect of interseismic stress accumulation must vary across the range. South of the high range, north-south horizontal compression rises during interseismic strain producing an increased Coulomb stress (Figure 7a). Farther north, where the maximum principal stress is vertical, the two effects compete. The increase of north-south compression has no effect on Coulomb stress since it approximately corresponds to the intermediate principal axis of the stress tensor (Figure 7b). However, east-west extension increases due to the divergence of thrusting along the arc contributing to a Coulomb stress increase (Figure 7c). This effect is more pronounced near the places where we have allowed the thrusting azimuth to vary. In these areas, the near vertical principal stress decreases slightly, contributing to a Coulomb stress decrease. It results in seismicity that becomes extinct generally above some elevation threshold between

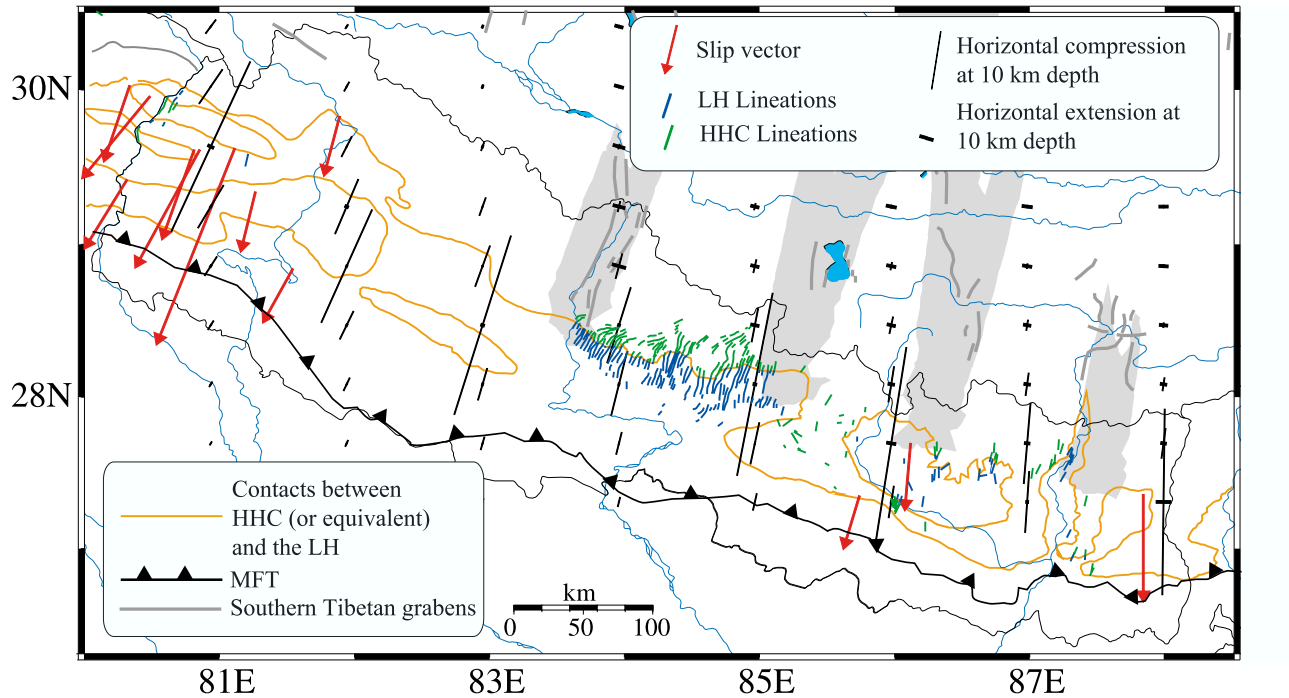

Figure 5. Slip vectors, interseismic strain rates ellipsoid, and mineral stretching lineations. Horizontal components of the strain rate ellipsoid were computed at 10 km depth from the model described in Figure 2. Slip vectors of moderate seismic events over the last 40 years are shown. Stretching lineations in the Himalayas (LH for lesser Himalaya, HHC for high Himalayan Cristalline) are from *Brunel* [1986] and *Pêcher* [1991] and from additional measurements in far western and central Nepal. Major normal faults in southern Tibet fall in a zone of more localized horizontal extension (shaded lobes correspond to horizontal extension rate in excess of 3.10^{-5}). Prolific seismicity near Mount Everest (87°E, 27.8°N) falls in a zone of decreased Coulomb stress (Figure 6). This is probably due to east-west stretching related to a change of thrusting azimuth that was not introduced in the model because it does not coincide with a major east-west graben. This seismicity is also close to the epicenter of the 1934 $Mw = 8.2$ earthquake. So, the pattern of east-west extension in the Himalayas is probably more distributed than predicted from our model or is time-dependent.

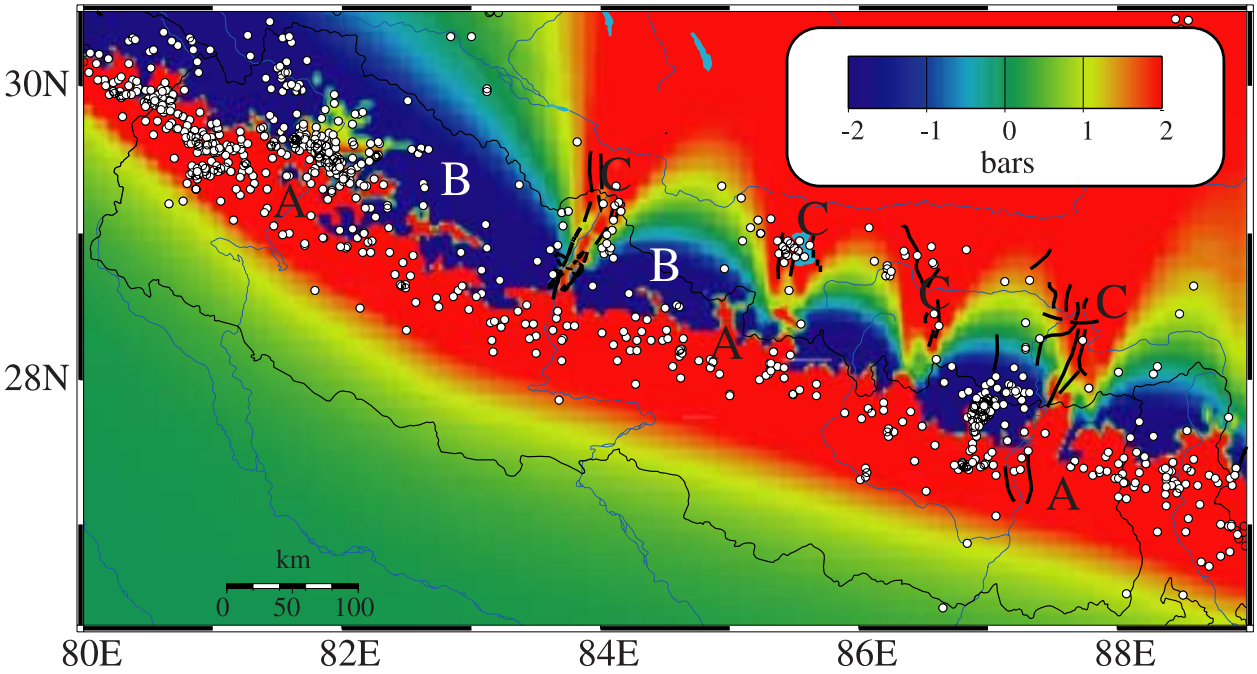

Figure 6. Coulomb stress variations computed for optimally oriented faults for a spatially varying regional stress field at 10 km depth. For the sake of simplicity we assume a vertical principal stress varying in proportion to elevation for a mean crustal density of 2900 g cm^{-3}, and the horizontal stresses are kept constant. This approximation neglects the effect of topography on horizontal stresses and tends to overestimate the variation of the deviatoric stresses with topography. Because topographic wavelengths shorter than about the typical 10 km depth of the seismicity are supported by elastic flexural stresses, σ_z was computed from a smoothed topography obtained by filtering the 30 s U.S. Geological Survey gtopo30 DEM using a Gaussian function with σ = 10 km. A, B, and C locate the different regional/interseismic stress patterns sketched in Figure 7.

grabens, and develops near the graben at higher east-west extension rates. Prominent features in the spatial distribution of seismicity can then be explained by this model. One of these features is the northward embayment in the seismicity of western Nepal, around 82°E. Our modeling implies that a $\sigma_{zz} \sim 70$ MPa increase of vertical stress, from the lesser Himalayas (~1000 m) to the tip of the grabens (~3500 m), is sufficient to shift from a stress state close to failure by north-south thrusting to one at the verge of failure by east-west extension. We infer at most 35 MPa deviatoric stresses in the zone of microseismic activity. Frictional slip on the MHT for such low deviatoric stresses implies a low frictional ranging of less than 0.1 for hydrostatic conditions, or 0.3 if a nearly lithostatic pore pressure is assumed. Such a low friction is consistent with the fact that the crustal wedge overrides the decollement below the Lesser Himalaya without any significant internal deformation [*Cattin and Avouac*, 2000].

5. Consistency Between Interseismic Strain, Coseismic Slip, and Long-Term Deformation Indicated by Stretching Lineations in the Lesser Himalaya and Extension North of the Himalaya

[7] The slip vectors of the moderate thrust events recorded along the front of the high Himalaya over the last about 40 yr might also be compared with the orientation of the maximum principal stress resulting from interseismic strain (Figure 5) because these earthquakes ruptured along shallow dipping thrust faults. The observed alignment between thrust events and the modeled orientation of σ_1 indicates that the deviatoric stresses at the front of the high range are consistent with long-term accumulation of current interseismic strain.

[8] Stretching lineations in the Lesser Himalaya can be used to provide some idea of the direction of tectonic transport over millions of years. Indeed, as deformation proceeds material is accreted to the Lesser Himalaya and ultimately exhumed, a process that has lead to the formation of duplexes in the Lesser Himalaya [*DeCelles et al.*, 2001; *Schelling and Arita*, 1991]. Lineations in the Lesser Himalaya are also parallel with the principal direction of compression induced by interseismic strain. These relationships in conjunction with a good match between modeled extensional stresses and the locations of north Himalayan grabens suggest that current interseismic strain is probably representative of the geologic transport directions over million years. Variations in the pattern of interseimic strain can only be subtle and/or transient. Deviatoric stresses are estimated to 20–30 MPa at front of the high range, and interseismic stresses accumulate at a rate of about 4–5 kPa/yr in this area [*Cattin and Avouac*, 2000]. It implies that if the recurrence interval of large Himalayan earthquakes is less than about 500 yr, stress variations associated with the seismic cycle amount to no more than 13% of ambient deviatoric stresses. Such small stress transfers between the seismogenic portion

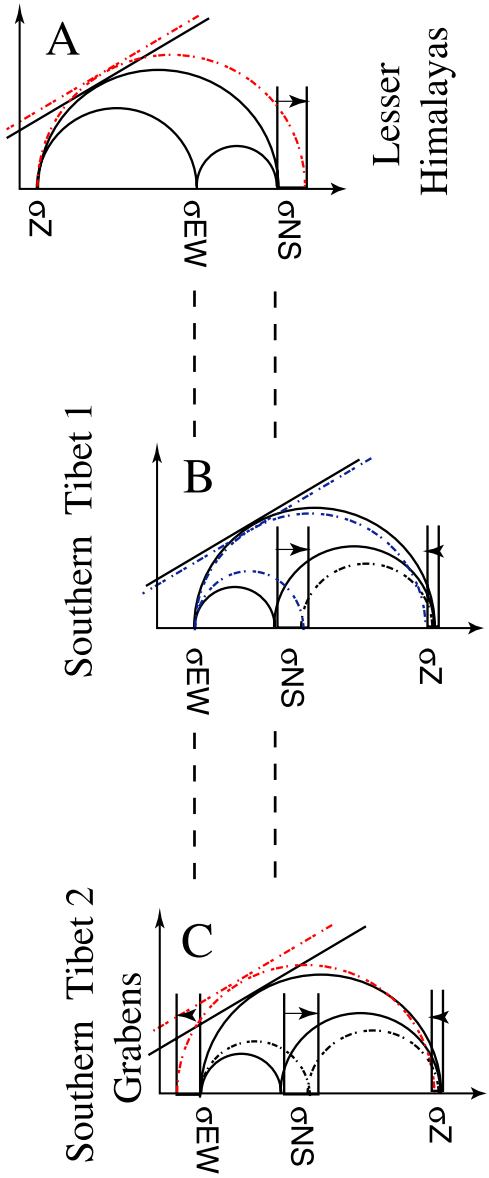

Figure 7. Variation of shear stress and normal stress associated with interseismic strain. The initial state is shown in black and is assumed tangent to the failure envelope represented by the straight line. A, B, and C refer to the different areas indicated in Figure 6. In area A, σ_1 is horizontal, striking about north-south and increasing during interseismic deformation, promoting failure. In area B, σ_1 is vertical and is reduced during interseismic strain so that failure should be inhibited. In area C, σ_3 is horizontal, striking approximately east-west and decreasing during interseismic deformation, promoting failure.

of the megathrust and its ductile downdip continuation, are consistent with relatively stationary strain during the interseismic period.

6. Conclusions and Implications

[9] The simple forward model of interseismic strain described above accounts for the distribution of background seismicity, coseismic slip vectors of moderate earthquakes, and geodetic displacements along the Nepal Himalaya. The topographic modulation of the stress field induces first-order heterogeneities in the microseismic cluster enabling us to quantify the deviatoric stresses at midcrustal depths. Strain must be rather uniform during a significant fraction of the interseismic period, and can be explained by a fully locked seismogenic zone, that extends from the MFT at the surface to beneath the front of the high range, over an average width of ~100 km along the ~1000 km long arc segment considered here. This means that the Himalayan megathrust mainly slips during transient events. Although recurring large earthquakes analogous to the 1934 Bihar Nepal event are probably dominant, transient aseismic events similar to those recently observed at places on subduction zones [*Dragert et al.*, 2001] might also contribute to this stress transfer. This suggests that a major earthquake along the seismic gap extending from Kathmandu area to Dehra Dun is highly plausible, but also suggests continuing efforts in seismic and geodetic monitoring. While we cannot rule out the presence of small heterogeneities given the scarcity of the GPS measurements and the uncertainties inherent in the campaign mode results, this study shows that large distinct asperities probably do not build during the interseismic phase on an intracontinental megathrust. How stresses are released during large Himalayan earthquakes is probably non unique and must depends on past seismic history as well as the stress field on the fault plane resulting from previous events, rather than on the pattern of accumulated stress in the interseismic period. Structural control on fault geometry and variations of physical properties probably influence rupture dynamics, so that the process might not actually be purely random.

[10] Stress variations during the seismic cycle on an intracontinental megathrust seem to be subtle, on the order of 10%, possibly due to the damping effect of the midcrustal ductile shear zone, leading to minor changes in the pattern and rate of interseismic strain. This strongly contrasts with some subduction zones where the stress field may vary over the seismic cycle from extension to compression [*Dmowska et al.*, 1996; *Lay et al.*, 1989] and along which significant postseismic afterslip may last for several decades inducing large geometric distortion of interseismic strain and reducing the seismic coupling factor [*Freymueller et al.*, 2000].

[11] **Acknowledgments.** We are most grateful to Yehuda Bock, Roger Bilham, and Jeffrey Freymueller for their comments and suggestions, which greatly helped improve this manuscript. This is Caltech Tectonics Observatory contribution number 8.

References

Baranowski, J., J. Armbruster, L. Seeber, and P. Molnar (1984), Focal depths and fault plane solutions of earthquakes and active tectonics of the Himalaya, *J. Geophys. Res.*, *89*, 6918–6928.

Bilham, R., K. Larson, J. Freymueller, and P. I. Members (1997), GPS measurements of present-day convergence across the Nepal Himalaya, *Nature*, *386*, 61–64.

Bilham, R., V. K. Gaur, and P. Molnar (2001), Himalayan seismic hazard, *Science*, *293*, 1442–1444.

Brunel, M. (1986), Ductile thrusting in the Himalayas: Shear sense criteria and stretching lineations, *Tectonics*, *5*, 247–265.

Cattin, R., and J.-P. Avouac (2000), Modeling of mountain building and the seismic cycle in the Himalaya of Nepal, *J. Geophys. Res.*, *105*, 13,389–13,407.

Chen, W. P., and H. Kao (1992), Seismotectonics of Asia: Some recent progress, in *The Tectonics of Asia*, edited by A. Yin and T. M. Harrison, pp. 37–62, Cambridge Univ. Press, New York.

DeCelles, P. G., D. M. Robinson, J. Quade, T. P. Ojha, C. N. Garzione, P. Copeland, and B. N. Upreti (2001), Stratigraphy, structure, and tectonic evolution of the Himalayan fold-thrust belt in western Nepal, *Tectonics*, *20*, 487–509.

Dmowska, R., G. Zheng, and J. R. Rice (1996), Seismicity and deformation at convergent margins due to heterogeneous coupling, *J. Geophys. Res.*, *101*, 3015–3029.

Dominguez, S., J.-P. Avouac, and R. Michel (2003), Horizontal coseismic deformation of the 1999 Chi-Chi earthquake measured from SPOT satellite images: Implications for the seismic cycle along the western foothills of central Taiwan, *J. Geophys. Res.*, *108*(B2), 2083, doi:10.1029/2001JB000951.

Dragert, H., K. Wang, and T. S. James (2001), A silent slip event on the deeper Cascadia subduction interface, *Science*, *292*, 1525–1528.

Freymueller, J. T., S. C. Cohen, and H. J. Fletcher (2000), Spatial variations in present-day deformation, Kenai Peninsula, Alaska, and their implications, *J. Geophys. Res.*, *105*, 8079–8101.

Hsu, Y.-J., N. Bechor, P. Segall, S.-B. Yu, L.-C. Kuo, and K.-F. Ma (2002), Rapid afterslip following the 1999 Chi-Chi, Taiwan earthquake, *Geophys. Res. Lett.*, *29*(16), 1754, doi:10.1029/2002GL014967.

Huang, B.-S. (2001), Evidence for azimuthal and temporal variations of the rupture propagation of the 1999 Chi-Chi, Taiwan earthquake from dense seismic array observations, *Geophys. Res. Lett.*, *28*, 3377–3380.

Hyndman, R. D., and K. Wang (1993), Thermal constraints on the zone of major thrust earthquake failure: The Cascadia subduction zone, *J. Geophys. Res.*, *98*, 2039–2060.

Jackson, M., and R. Bilham (1994), Constraints on Himalayan deformation inferred from vertical velocity fields in Nepal and Tibet, *J. Geophys. Res.*, *99*, 13,897–13,912.

Johnson, K. M., Y.-J. Hsu, P. Segall, and S.-B. Yu (2001), Fault geometry and slip distribution of the 1999 Chi-Chi, Taiwan earthquake imaged from inversion of GPS data, *Geophys. Res. Lett.*, *28*, 2285–2288.

Jouanne, F., J.-L. Mugnier, M. Pandey, J. F. Gamond, P. Le Fort, L. Serrurier, C. Vigny, J.-P. Avouac, and IDYLHIM Members (1999), Oblique convergence in the Himalayas of western Nepal deduced from preliminary results of GPS measurements, *Geophys. Res. Lett.*, *26*, 1933–1936.

Jouanne, F., J.-L. Mugnier, J. F. Gamond, P. Le Fort, M. R. Pandey, L. Bollinger, M. Flouzat, and J.-P. Avouac (2004), Current shortening across the Himalayas of Nepal, *Geophys. J. Int.*, *157*, 1–14, doi:10.1111/j.1365-246X.2004.02180.x.

King, G. C. P., R. S. Stein, and J. Lin (1994), Static stress changes and the triggering of earthquakes, *Bull. Seismol. Soc. Am.*, *84*, 935–953.

Larson, K., R. Bürgmann, R. Bilham, and J. T. Freymueller (1999), Kinematics of the India-Eurasia collision zone from GPS measurements, *J. Geophys. Res.*, *104*, 1077–1093.

Lavé, J., and J.-P. Avouac (2000), Active folding of fluvial terraces across the Siwaliks Hills, Himalayas of central Nepal, *J. Geophys. Res.*, *105*, 5735–5770.

Lay, T., and H. Kanamori (1981), An asperity model of large earthquake sequences, in *Earthquake Prediction: An International Review*, *Maurice Ewing Ser.*, vol. 4, edited by D. W. Simpson and P. G. Richards, pp. 579–592, AGU, Washington, D. C.

Lay, T., L. Astiz, H. Kanamori, and D. H. Christensen (1989), Temporal variation of large interplate earthquakes in coupled subduction zones, *Phys. Earth Planet. Inter.*, *54*, 258–312.

Mazzotti, S., X. Le Pichon, P. Henry, and S. I. Miyazaki (1999), Full interseismic locking of the Nankaıuml; and Japan-West Kurile subduction zones: An analysis of uniform elastic strain accumulation in Japan constrained by permanent GPS, *J. Geophys. Res.*, *105*, 13,159–13,177.

Molnar, P., and W. P. Chen (1983), Focal depths and fault plane solutions of earthquakes under the Tibetan plateau, *J. Geophys. Res.*, *88*, 1180–1196.

Molnar, P., and H. Lyon-Caen (1989), Fault plane solutions of earthquakes and active tectonics of the Tibetan plateau and its margins, *Geophys. J. Int.*, *99*, 123–153.

Nakata, T. (1989), Active faults of the Himalaya of India and Nepal, in *Tectonics of the Western Himalayas*, edited by L. L. Malinconico Jr. and R. Lillie, pp. 243–264, Geol. Soc. of Am., Boulder, Colo.

Ni, J., and M. Barazangi (1984), Seismotectonics of the Himalayan collision zone: Geometry of the underthrusting Indian plate beneath the Himalaya, *J. Geophys. Res.*, *89*, 1157–1163.

Okada, Y. (1992), Internal deformation due to shear and tensile faults in a half space, *Bull. Seismol. Soc. Am.*, *82*, 1018–1040.

Oleskevich, D. A., R. D. Hyndman, and K. Wang (1999), The updip and downdip limit to great subduction earthquakes: Thermal and structural models of Cascadia, south Alaska, SW Japan and Chile, *J. Geophys. Res.*, *104*, 14,965–14,991.

Pandey, M. R., R. P. Tandukar, J.-P. Avouac, J. Lavé, and J. P. Massot (1995), Interseismic strain accumulation on the Himalaya crustal ramp (Nepal), *Geophys. Res. Lett.*, *22*, 741–754.

Pandey, M. R., R.-P. Tandukar, J. P. Avouac, J. Vergne, and T. Héritier (1999), Seismotectonics of Nepal Himalayas from a local seismic network, *J. Asian Earth Sci.*, *17*, 703–712.

Pêcher, A. (1991), The contact between the higher Himalaya cristallines and the Tibetan sedimentary series: Miocene large-scale dextral shearing, *Tectonics*, *10*, 587–598.

Prawirodirdjo, L., Y. Bock, R. McCaffrey, J. Genrich, E. Calais, C. Stevens, S. S. O. Puntodewo, C. Subarya, J. Rais, P. Zwick, and Fauzi (1997), Geodetic observations of interseismic strain segmentation at the Sumatra subduction zone, *Geophys. Res. Lett.*, *24*, 2601–2604.

Savage, J. C. (1983), A dislocation model of strain accumulation and release at a subduction zone, *J. Geophys. Res.*, *88*, 4984–4996.

Schelling, D., and K. Arita (1991), Thrust tectonics, crustal shortening and the structure of the Far Eastern Nepal Himalaya, *Tectonics*, *10*, 851–862.

Vergne, J., R. Cattin, and J. P. Avouac (2001), On the use of dislocations to model interseismic strain and stress build-up at intracontinental thrust fault, *Geophys. J. Int.*, *147*, 155–162.

Zhao, W., K. D. Nelson, and P. I. Team (1993), Deep seismic-reflection evidence continental underthrusting beneath southern Tibet, *Nature*, *366*, 557–559.

J. P. Avouac, Geological and Planetary Sciences Division, California Institute of Technology, Pasadena, CA 91125, USA. (avouac@gps.caltech.edu)

L. Bollinger, CEA, Laboratoire Détection et Géophysique, F-91680 Bruyères le Châtal, France. (laurent.bollinger@cea.fr)

R. Cattin, Laboratoire de Géologie, Ecole Normale Supérieure, 24 rue Lhomond, F-75005 Paris, France. (cattin@opale.ens.fr)

M. R. Pandey, Department of Mines and Geology, National Seismic Centre, Lainchur, Kathmandu, Nepal. (nscdmg@mos.com.np)